Evaluation of multispectral middle infrared aircraft images for lithologic mapping in the East Tintic Mountains, Utah

Anne B. Kahle
Jet Propulsion Laboratory, California Institute of Technology
Pasadena, California 91103

Lawrence C. Rowan
U.S. Geological Survey
Reston, Virginia 22092

ABSTRACT

Six channels of multispectral middle infrared (8 to 14 μm) aircraft scanner data were acquired over the East Tintic mining district, Utah. This area has high relief and moderate vegetation and consists mainly of Tertiary silicic igneous rocks and Paleozoic quartzite and carbonate rocks that have been locally hydrothermally altered. These digital-image data were computer processed to create a color-composite image based on principal component transformations. Color differences in this image are related to the spectral differences in the surface material and allow discrimination of several rock types, depending primarily on their silica content. When combined with a visible and near infrared color-composite image from a previous flight, with limited field checking, it is possible to discriminate quartzite, carbonate rocks, quartz latitic and quartz monzonitic rocks, latitic and monzonitic rocks, silicified altered rocks, argillized altered rocks, and vegetation.

INTRODUCTION

Laboratory measurements of middle infrared (MIR) (5 to 40 μm) spectra of rocks and minerals show many diagnostic features. The region between 8 and 14 μm holds the most promise for remote sensing because this is an excellent atmospheric window and is also the region of maximum thermal emission at terrestrial surface temperatures. Within this spectral range, the most prominent spectral features are due to silicon-oxygen stretching vibrations. These features change location and intensity with varying composition and structure (Hunt and Salisbury, 1974, 1975, 1976; Vincent and others, 1975). Lyon (1965) indicated that these intense features (known as reststrahlen bands in reflectance spectra) shift to shorter wavelengths as silica content increases.

The possibility of exploiting these spectral features for remote sensing of rock type from aircraft or satellite has been suggested by many authors (Vickers and Lyon, 1967; Vincent and Thomson, 1972; Vincent, 1975). However, owing to lack of adequate multispectral scanners (Vincent, 1975), very few tests of the technique have been possible. Hovis and others (1968) concluded, from a nonimaging emittance spectrometer flight over desert terrain in California, that even though atmospheric effects were significant, the reststrahlen bands of silicates were observable. With nonimaging spectrometer data from a flight over the Pisgah Crater, California, lava flows and surroundings, Lyon (1972) was able to distinguish between the basalts, the alluvial fans, and the windblown sands and also recognized spectral differences within the basalt flows. Two tests using a two-channel imaging spectrometer have been reported. Vincent and others (1972) used a scanner having a bandpass between 8.2 and 10.9 μm and another bandpass between 9.4 and 12.1 μm over a sand quarry near Mill Creek, Oklahoma. Using a ratio method on the spatially registered images, they produced images on which they could distinguish between the quartz sand or sandstone and the nonsilicate surface material. Vincent and Thomson (1972), using the same scanner over the Pisgah Crater area, were able to distinguish dacite from basalt and rhyolitic tuff from the surrounding alluvium. However, until now the lack of adequate imaging multispectral scanners has precluded further validation of the use of spectral emittance data gathered from aircraft.

Recently we acquired multispectral MIR (8 to 13 μm) scanner data of the East Tintic Mountains in central Utah from the now-defunct Bendix 24-channel scanner, flown on the NASA C-130 aircraft. These data consist of six channels of calibrated scanner images of moderate spectral resolution (0.5 to 1.0 μm bandwidth), available in digital format on computer-compatible tapes. Results obtained during this flight provided an unprecedented opportunity to analyze multispectral MIR image data in a geologically complex area. The dis-

GEOLOGY, v. 8, p. 234–239, MAY 1980

trict, in an area of high relief and moderate vegetation, consists mainly of Tertiary silicic igneous rocks and Paleozoic quartzite and carbonate rocks that have been locally hydrothermally altered.

The purpose of this paper is to demonstrate that, with the aid of suitable image-processing techniques and sufficient field verification, a significant amount of geologic information can be derived for such an area from MIR multispectral images.

MIDDLE INFRARED SPECTRA OF ROCKS

In the past, as discussed by Lyon (1962), laboratory measurements of the MIR spectra of minerals have shown that many diagnostic features exist in this spectral range. Recognizing that for remote sensing applications we must consider the spectra of rocks, not minerals, Coblentz (1905), Lyon (1964), Hunt and Salisbury (1974, 1975, 1976), and Vincent and others (1975) have measured and published rock spectra. Although, in general, these spectra tend to be somewhat predictable on the basis of the spectra of the constituent minerals, molecular interactions are present that tend to mask and distort some features (Hunt and Salisbury, 1974).

Laboratory spectra are usually determined for carefully prepared specimens under conditions that tend to maximize the spectral information. Generally, these measurements are made either in the transmission or the reflection mode. Emission spectra are more difficult to measure, being very sensitive to sample conditions such as particle size and near-surface temperature gradients. They are often obtained indirectly, by applying Kirchoff's law to reflectance spectra (Lyon, 1965). Despite these drawbacks we do use laboratory spectra as a key to the interpretation of remotely sensed multispectral emission data. The most complete set of laboratory spectra of rocks available for the MIR are the transmission spectra of Hunt and Salisbury (1974, 1975, 1976).

In Figure 1, we show a few laboratory transmission spectra from Hunt and Salisbury (1974, 1975, 1976). These are representative of spectra for most of the rock types found in the East Tintic area and illustrate the features most often considered likely to be detected by remote sensing. In the silicate rocks (quartzite, quartz monzonite, monzonite, latite, olivine basalt), the broad, deep decrease in transmission between 8 and 11 μm has been identified by Hunt and Salisbury as being due to Si-O stretching vibrations. The depth and position of the band have been shown to be related to the structure of the constituent minerals and are especially sensitive to the quartz content of the rocks. In the carbonate rocks (limestone, dolomite), the most prominent feature is the C-O asymmetric stretch which, near 7 μm, lies outside the 8- to 14-μm atmospheric window. Throughout this window region, the carbonate spectra are almost flat or show a gradual rise except for the narrow out-of-plane bending feature near 11.5 μm. Spectral features between 8 and 14 μm in the clays (kaolinite and montmorillonite) are ascribed by Hunt and Salisbury to various Si-O-Si and Si-O stretching vibrations and an Al-O-H bending mode. The montmorillonite features are less distinct than those in the kaolinite, because the numerous exchangeable cations and water molecules in the montmorillonite structure allow many different vibrations. Near the center of Figure 1, we show a spectrum of a rock typical of many in the East Tintic area—a limestone containing clay and quartz—which shows spectral features from each of these components.

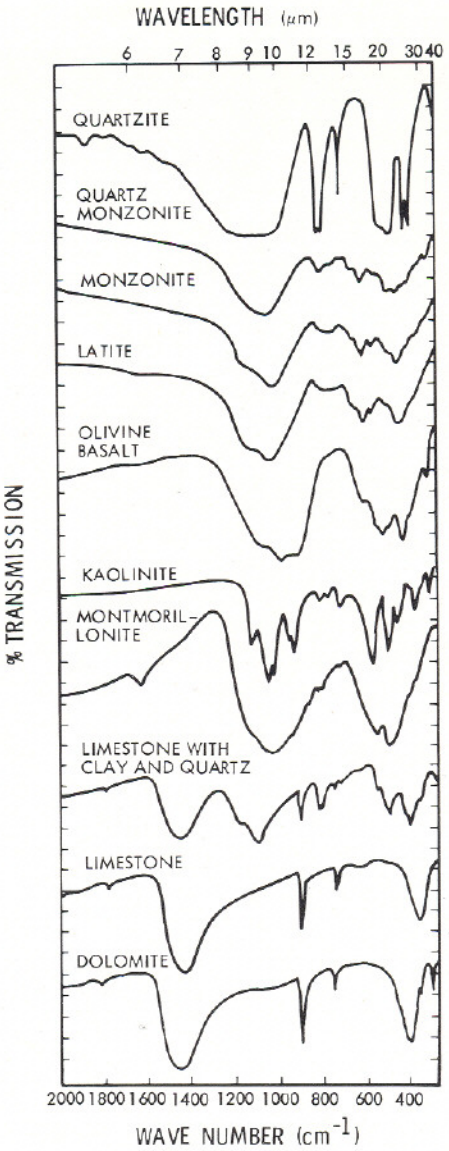

Figure 1. Laboratory transmission spectra of some rocks and minerals (after Hunt and Salisbury, 1974, 1975, 1976).

Considering the complexity of the spectral signatures and the only subtle differences between some of them, it is not immediately apparent whether use of moderately broadband (0.5- to 1.0-μm width) multispectral sensors in the MIR will enable us to discriminate between any surface material other than perhaps silicates versus nonsilicates.

GEOLOGIC SETTING

The East Tintic Mountains, Utah, are a generally north-trending block-faulted range consisting of complexly folded and faulted Paleozoic sedimentary rocks that are partly covered by Tertiary volcanic rocks. Clastic rocks dominate the lower one-third of the 9,000-m-thick Paleozoic section, whereas carbonate rocks with subordinate amounts of shale and clastic rocks predominate in the remainder (Morris and Lovering, 1961, 1979; Morris, 1964a, 1964b). The Tertiary volcanic rocks—mainly tuffs, flows, and agglomerates—are of quartz latitic and latitic composition. Emplacement of related monzonite, biotite monzonite, and quartz monzonite porphyry bodies resulted in several types of altered rocks.

In order to evaluate the multispectral MIR images for distinguishing lithologic variations, a map showing the general distribution of the principal rock types was compiled from the 1:24,000-scale geologic maps of the area (Morris, 1964a, 1964b; Fig. 2). Seven unaltered and silicified altered rock types along with vein deposits are shown, and alluvium, a mixture of these two broad categories, is also shown (Fig. 2).

The main consideration in compiling this map was the amount of quartz present, because initial examination of the individual black-and-white spectral-emittance images indicated that the intense absorption band centered near 9.2 μm, which is characteristic of quartz, was a dominant feature. Therefore, the Paleozoic sedimentary rocks were categorized in three lithologic units: (1) quartzite, sandstone, shale, and quartzose conglomerate; (2) limestone and dolomite; and (3) interbedded arenaceous and carbonate rocks. Limestone and dolomite were not

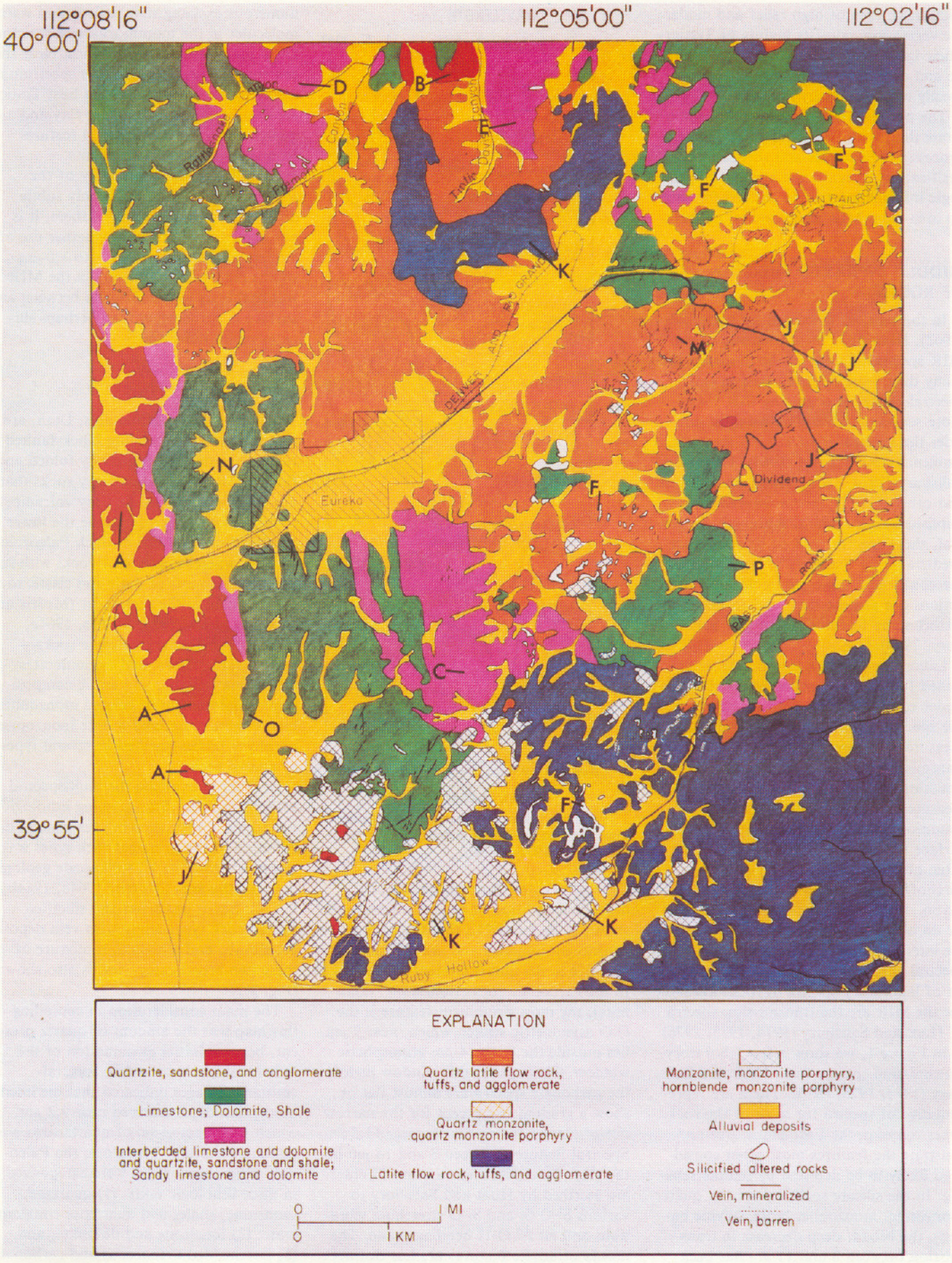

Figure 2. Generalized lithologic map of the central part of the East Tintic Mountains, Utah (after Morris, 1964a, 1964b). See Figure 3 caption for letter code.

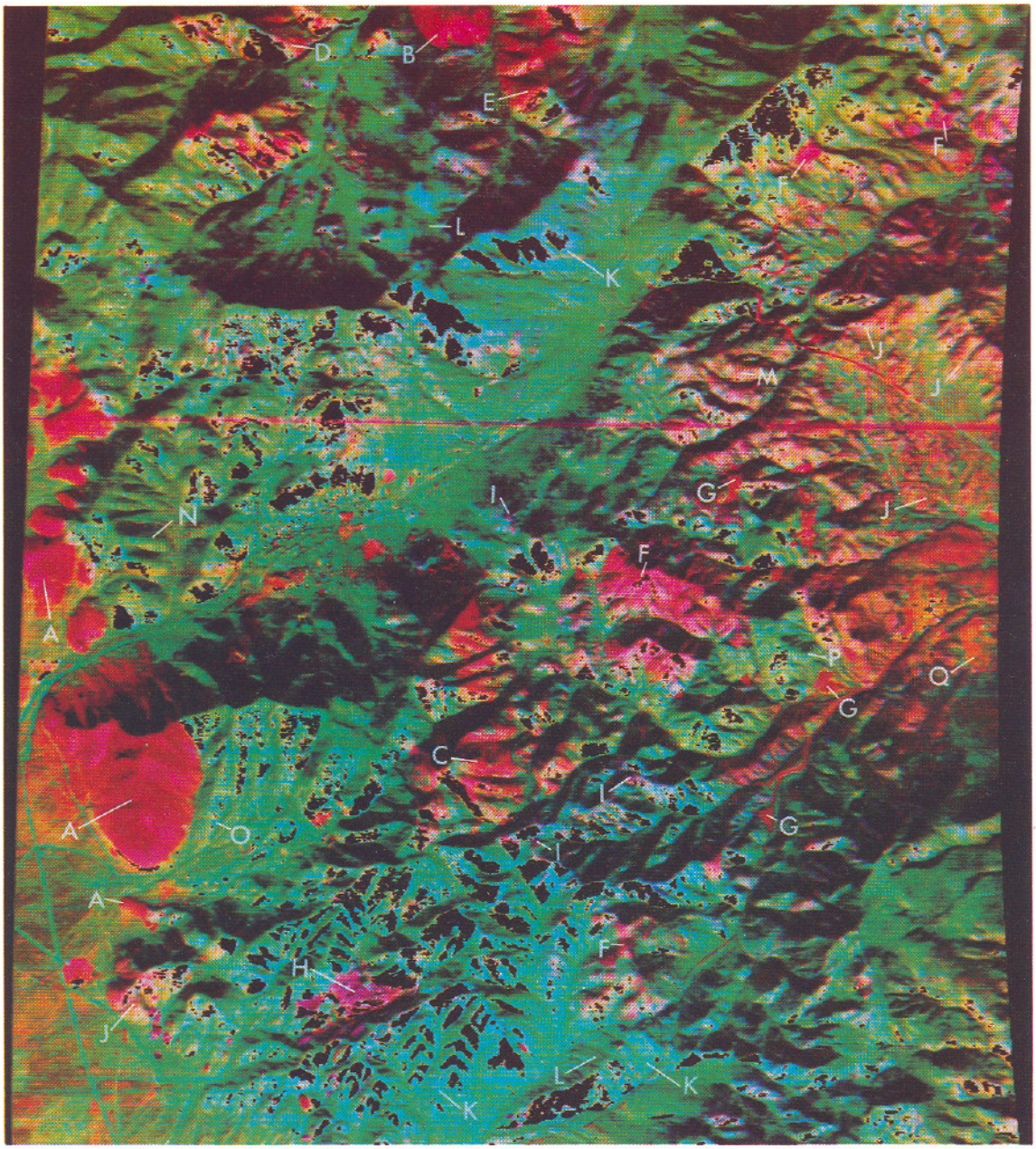

Figure 3. Color-composite image of the East Tintic Mountains, Utah, based on principal component transformations of MIR multispectral data. A, B = quartzite; C, D, E = interbedded sandstone, limestone, quartzite, shale, dolomite, and chert; F = silicified rocks; G = mine areas; H = Dragon mine; I = argillized rocks; J = quartz latite and quartz monzonite; K = latite and monzonite; L = vegetated areas; M = calcitic quartz latite; N, O = carbonate rocks; P = hydrothermal dolomite; Q = mine tailings and ponds.

treated separately because their emittance spectra are very similar in the 8- to 14-μm region. However, as laboratory spectra indicate (Fig. 1), the presence of quartz as an impurity in carbonate rocks gives rise to an absorption band centered near 9.2 μm (Hunt and Salisbury, 1975).

The Tertiary volcanic and related intrusive rocks were categorized according to the presence or absence of quartz as a primary constituent. Quartz latitic rocks are widespread in the northern part of the study area, but their intrusive equivalent is restricted to the Swansea Quartz Monzonite porphyry near the western boundary of the study area and to a few scattered dikes (Fig. 2). Rocks of latitic composition are predominant in the southeastern and north-central parts, and related intrusive rocks are widespread in the southwestern part and as small intrusive bodies distributed along a northeast-trending zone across the central region (Fig. 2).

Hydrothermally altered rocks have been placed in categories: (1) silicified rocks in which the volume percent of quartz is greater than the weight percent of SiO_2 of the original rock and in which alunite, kaolinite, and K-mica are common; (2) argillized rocks that contain abundant quartz, kaolinite, alunite, halloysite, montmorillonite, and K-mica; (3) calcitic volcanic rocks in which calcite replaces plagioclase phenocrysts; and (4) hydrothermal dolomite in which calcite is converted to dolomite (Lovering, 1949). In addition, the intrusive bodies are locally altered.

Morris (1964a, 1964b) mapped the

distribution of silicified rocks throughout the study area (Fig. 2), but the other altered rocks have been mapped only in the East Tintic mining district (Lovering, 1949). However, the distribution of the most widespread type, argillized rocks, is generally known from analysis of Landsat and aircraft visible and near infrared (NIR) color-ratio composite images (Rowan and Abrams, 1978a, 1978b). The other three altered rock types are not detectable in these images.

IMAGE DATA PROCESSING

The six channels of aircraft data (8.3 to 8.7 μm, 8.8 to 9.3 μm, 9.4 to 9.9 μm, 10.1 to 11.0 μm, 11.0 to 12.0 μm, and 12.0 to 13.0 μm) were contrast enhanced and displayed as black and white images. Because the radiance emitted from the surface is highly dependent upon surface temperature, these images were dominated by temperature (and hence topography). Display of the much more subtle spectral emissivity differences between the channels due to variations in the surface materials required more elaborate image processing.

Using onboard calibration, a simple atmospheric model, and an assumed constant surface emittance of 0.93 in the 11- to 12-μm range, we derived a surface-temperature image from the 11- to 12-μm radiance data. (The 12- to 13-μm data were not used to derive a temperature because of excessive noise.) We could then derive surface-emittance images for the remaining four channels between 8 and 11 μm.

Several additional images were prepared from the multispectral radiance and emittance data, including color composites, ratios, color-ratio composites, and principal component transformations. The most satisfactory image product for separation of rock types (Fig. 3) was produced from the radiance data in channels 8.27 to 8.7 μm, 8.8 to 9.3 μm, and 10.1 to 11.0 μm. The color-enhancement procedure consisted of a nonlinear transformation in which each of the three output channels forming the final color triplet was a function of all three input values. The transformation consists logically of a principal component rotation, followed by "Gaussian" contrast enhancement and then by an inverse rotation (actually performed by table lookup). This transformation was chosen to remove the correlation that existed between the original components, thus fully utilizing the available color range. (For a more detailed description of the image processing, see Kahle and others, 1979). A useful feature of the final display is that, although emittance differences appear as variations in color, the intensity of any element of the enhanced scene remains a function of local temperature, just as for the original components. Because temperature is largely topographically controlled, these intensity variations reflect local topography, thus aiding interpretation. Unfortunately, the original radiance data contained some areas where the ground temperature was either too hot or too cold to lie within the range of the recording system. These areas are shown in black in Figure 3.

EVALUATION OF MIDDLE INFRARED COLOR COMPOSITE IMAGE

Evaluation of the MIR color composite image was conducted by comparing the distribution of colors in the image (Fig. 3) with the occurrence of rock units in the generalized map (Fig. 2) and by field checking critical areas. In general, areas shown as red to pink and purple in the image are underlain by rocks in which quartz is a major constituent, whereas blue and green represent rocks that have minor quartz content; green also represents dense vegetation.

The most vivid red areas in the image along the western border and in the north-central part (A, B in Figs. 2, 3) represent quartzite. Slightly less intense and uniform red areas in the central part of the study area and both east and west of the quartzite in the north (C, D, and E, respectively, in Figs. 2, 3) consist of interbedded sandstone, limestone, quartzite, shale, dolomite, and chert.

Silicified altered rocks also appear red to pink in the image (F in Figs. 2, 3). Note that at Big Hill (the large pink unit near the center of the image) on the lithologic map (Fig. 2), only a few silicified outcrops are shown, but in the scanner image (Fig. 3), the entire area is bright pink. Field checking indicates that the silicified rocks are much more widespread than mapped, and debris from them covers the entire hill.

Many small red areas correspond to mine dumps and cleared ground around mines (G in Fig. 3), all of which have a high quartz content. The largest exposed mine area, the Dragon mine (H in Fig. 3), is exceptional, however, in that it is purple in the image and has a high clay content (halloysite; Morris and Lovering, 1961). Several other areas of argillized rocks have a similar appearance (I in Fig. 3). These differences in color may suggest that the red areas indicate the presence of large amounts of quartz, whereas the purple denotes higher proportions of clay minerals.

One of the most surprising contrasts seen in the MIR color-composite image is the separation of quartz latitic–quartz monzonitic rocks from latitic-monzonitic rocks: the former unit appears pink (J in Figs. 2, 3), whereas the latter unit is blue (K in Figs. 2, 3). Important exceptions occur where the rocks are argillized or silicified and, hence, appear purple or red, or where vegetation is dense, in which case the area is green (L in Fig. 3). Calcitic quartz latitic rocks (Lovering, 1949) also appear pink (M in Figs. 2, 3), which might be expected because the quartz content was not affected by the alteration process and the calcite has been leached from the surface.

Carbonate rocks generally appear green in the color composite image (N in Figs. 2, 3). In some places, however, they are blue or blue-green (O in Fig. 3) and, therefore, similar to the latitic-monzonitic rocks (K in Figs. 2, 3). Preliminary field examination suggests that the blue and blue-green areas correspond to high proportions of sandy soil. Hydrothermal dolomite (Lovering, 1949) is compositionally similar to unaltered dolomitic rocks in the study area and, therefore, also appears green and blue-green in the image (P in Figs. 2, 3).

Mining and milling operations in the east-central part of the area appear bright yellow in the image (Q in Fig. 3).

DISCUSSION

The image-processing procedures used to generate Figure 3, although chosen to maximize the differences among surface materials, make it difficult to relate the image color to these spectral differences. However, some general relationships can be noted. Red is consistently related to the presence of quartz-bearing rocks and, therefore, implies an intense absorption band centered between 8 and 10 μm as expected for quartz (see Fig. 1). In contrast, green appears to represent generally spectrally flat materials such as carbonate rocks and vegetation. In general, the blue correlates with latite and monzonite, both silicate rocks but without quartz as a major constituent.

Examination of spectral-emittance curves derived from the image data suggests that the principal difference we are seeing among the surface materials is in the depth of the spectral features and that

variations in the position of the absorption band used in other areas to distinguish among silicate materials (Vincent and Thomson, 1972) appear to be less important here. These results suggest that both intensity and position of the spectral bands need to be studied.

Some distinctions that are not possible in these MIR images can be made in visible and NIR color-ratio composite images that were previously produced from NASA 24-channel scanner data specifically for mapping hydrothermally altered rocks (Rowan and Abrams, 1978b) and vegetation distribution (Milton and Madura, 1980). Although both carbonate rocks and vegetation lack significant absorption bands in the 8- to 12-μm region, the fact that they are readily distinguishable in the visible and NIR color-ratio composite images allows mapping of the carbonate rocks. Argillized rocks and quartz latitic rocks are not consistently distinguishable in the MIR image but are clearly separable in the visible and NIR image, owing to their spectral contrast in the 2.2-μm region. Thus, use of color-composite images from both the MIR and the visible and NIR, combined with limited field checking, permit mapping of quartzite, carbonate rocks, quartz latitic and quartz monzonitic rocks, latitic and monzonitic rocks, silicified altered rocks, and argillized altered rocks.

These results indicate that multispectral MIR data have considerable potential for distinguishing certain rock types. However, more work is needed in areas of other rock types in order to evaluate this approach to lithologic mapping. Another important consideration in extending this technique to satellite-borne sensors is the effect of an ozone band centered near 9.65 μm. To the best of our knowledge, no adequately equipped multispectral scanner is now in operation, nor do any other Bendix 24-channel scanner digital MIR data exist for areas of geologic interest. Construction of a new scanner is needed for continuing these studies.

REFERENCES CITED

Coblentz, W. W., 1905, Investigations of infrared spectra: Carnegie Institution of Washington Publication, no. 35.

Hovis, W. A., Jr., Blaine, L. R., and Callahan, W. R., 1968, Infrared aircraft spectra over desert terrain 8.5 μ to 16 μ: Applied Optics, v. 7, p. 1137–1140.

Hunt, G. R., and Salisbury, J. W., 1974, Mid-infrared spectral behavior of igneous rocks: Cambridge, Mass., U.S. Air Force Cambridge Research Laboratories Technical Report AFCRL-TR-74-0625.

——1975, Mid-infrared spectral behavior of sedimentary rocks: Cambridge Mass., U.S. Air Force Cambridge Research Laboratories Technical Report AFCRL-TR-75-0356.

——1976, Mid-infrared spectral behavior of metamorphic rocks: Cambridge, Mass., U.S. Air Force Cambridge Research Laboratories Technical Report AFCRL-TR-76-0003.

Kahle, A. B., Madura, D. P., and Soha, J. M., 1979, Processing of multispectral thermal IR data for geological applications: Pasadena, California Institute of Technology, Jet Propulsion Laboratory Publication 79-89.

Lovering, T. S., 1949, Rock alteration as a guide to ore—East Tintic district, Utah: Economic Geology Monograph 1, 65 p.

Lyon, R.J.P., 1962, Minerals in the infrared—A critical bibliography: Menlo Park, Calif., Stanford Research Institute, 76 p.

——1964, Evaluation of infrared spectrophotometry for compositional analysis of lunar and planetary soils, Part II: Rough and powdered surfaces: National Aeronautics and Space Administration Contractor Report CR-100, 172 p.

——1965, Analysis of rocks by spectral infrared emission (8 to 25 microns): Economic Geology, v. 60, p. 715–736.

——1972, Infrared spectral emittance in geological mapping: Airborne spectrometer data from Pisgah Crater, California: Science, v. 175, p. 983–986.

Milton, N. M., and Madura, D. P., 1980, Vegetation distribution of the central part of the East Tintic Mountains, Utah: U.S. Geological Survey Miscellaneous Field Studies Map 1195 (in press).

Morris, H. T., 1964a, Geology of the Eureka quadrangle, Utah and Juab Counties, Utah: U.S. Geological Survey Bulletin 1142-K, 29 p.

——1964b, Geology of the Tintic Junction quadrangle, Tooele, Juab, and Utah Counties, Utah: U.S. Geological Survey Bulletin 1142-L, 23 p.

Morris, H. T., and Lovering, T. S., 1961, Stratigraphy of the East Tintic Mountains, Utah: U.S. Geological Survey Professional Paper 361, 145 p.

——1979, General geology and mines of the East Tintic mining district, Utah and Juab Counties, Utah: U.S. Geological Survey Professional Paper 1024, 203 p.

Rowan, L. C., and Abrams, M. J., 1978a, Evaluation of Landsat multispectral scanner images for mapping altered rocks in the East Tintic Mountains, Utah: U.S. Geological Survey Open-File Report 78-736, 73 p.

——1978b, Mapping hydrothermally altered rocks in the East Tintic Mountains using 0.4–2.38 μm multispectral scanner aircraft images: International Association on the Genesis of Ore Deposits Meeting, Alta, Utah, Program and Asbtracts, p. 156.

Vickers, R. S., and Lyon, R.J.P., 1967, Infrared sensing from spacecraft: A geological interpretation, *in* Heller, G. B., ed., Thermophysics of spacecraft and planetary bodies. Radiation properties of solids and the electromagnetic radiation environment in space: New York, Academic Press, Inc., p. 585–607.

Vincent, R. K., 1975, The potential role of thermal infrared multispectral scanners in geologic remote sensing: Institute of Electrical and Electronic Engineers Proceedings, v. 63, p. 137–147.

Vincent, R. K., and Thomson, F., 1972, Spectral compositional imaging of silicate rocks: Journal of Geophysical Research, v. 77, p. 2465–2472.

Vincent, R. K., Thomson, F., and Watson, K., 1972, Recognition of exposed quartz sand and sandstone by two-channel infrared imagery: Journal of Geophysical Research, v. 77, p. 2473–2477.

Vincent, R. K., and others, 1975, Thermal-infrared spectra and chemical analyses of twenty-six igneous rock samples: Remote Sensing of Environment, v. 4, p. 199–209.

ACKNOWLEDGMENTS

Reviewed by G. R. Hunt and R. K. Vincent. We thank D. Madura for processing the images and A.F.H. Goetz and K. Watson for reading the manuscript. This paper presents the results of one phase of research carried out at the Jet Propulsion Laboratory, California Institute of Technology, under Contract NAS7-100, sponsored by the National Aeronautics and Space Adminstration.

MANUSCRIPT RECEIVED OCT. 29, 1979

MANUSCRIPT ACCEPTED FEB. 25, 1980